



# Study of Saudi Arabian climatic conditions using Hurst exponent and climatic predictability index

Shafiqur Rehman \*

*Engineering Analysis Section, Center for Engineering Research, Research Institute,  
King Fahd University of Petroleum and Minerals, P.O. Box 767, Dhahran-31261, Saudi Arabia*

Accepted 2 January 2007

---

## Abstract

This paper utilizes Hurst exponent to study the persistency of meteorological parameters individually and dependency of rainfall/precipitation on pressure and temperature using climate predictability index. For the purpose, daily averages of surface pressure and temperature and daily total rainfall data for a period of 7 years for three locations and 14 years for seven locations has been utilized. The Hurst exponents ( $H$ ) for above mentioned meteorological parameters were calculated using rescaled range analysis ( $R/S$ ) and absolute moments methods. These  $H$  values were used to calculate the fractal dimension  $D$  for pressure, temperature and rainfall data. Finally, these  $D$ 's were used to calculate the climate predictability index  $PI_C$  in terms of pressure predictability index ( $PI_P$ ), temperature predictability index ( $PI_T$ ) and rainfall predictability index ( $PI_R$ ). The Hurst exponent analysis showed that  $H$  values for rainfall, relative humidity and wind speed time series data for all the stations were  $>0.5$  which is indicative of persistence behavior of the parameters on the previous values while for pressure and temperature  $H$  values were  $<0.5$  means anti-persistence behavior. The climate predictability index showed that in most of the cases the rainfall was dependent on both pressure and temperature predictability indices. In some cases it was more dependent on pressure index than the temperature and in some cases otherwise. In Saudi Arabia there is no prevalent or established rainy season and the present analysis could not result into concrete results. It is therefore recommended to analyze the data by breaking the entire data set into seasons and further into different years.

© 2007 Elsevier Ltd. All rights reserved.

---

## 1. Introduction

Weather plays a critical role in the life cycle of all human beings, hence should be understood well. Ever since it was first realized that humanity is capable of changing its natural surroundings more rapidly than nature can repair it, model-based predictions about climate change has been one of the main research areas in science as stated by Kurnaz [1]. Nature provides different forms of data which can be converted to climatic data. For example, tree ring history from Scandinavia indicates that there was a period of high temperatures between 9th and 13th centuries, called the Medieval

---

\* Tel.: +966 3 8603802; fax: +966 3 8603996.

E-mail address: [srehman@kfupm.edu.sa](mailto:srehman@kfupm.edu.sa)

URL: <http://faculty.kfupm.edu.sa/ri/srehman>.

Warm Period, [1]. The tree ring temperature history for this period agrees with the glacier data, and has been supported by the historical records of Norse seafaring and colonization around the North Atlantic at the end of the 9th century. The weather forecast to first approximation is a rather simple issue. A cold day is usually followed by a cold day, and a warm day is usually followed by a warm day.

With the introduction of modern technologies such as digital image processing, finite element analysis, digital satellite mapping, and powerful computer simulation programs, the amount of data available to researchers and scientists has grown to immense proportions. Unfortunately, the development of technology to acquire data has far outpaced the development of technology to read, store, transmit and utilize the data. The storage and communication difficulties associated with the FBI's fingerprint files are popular examples [2–5]. However, even if today's computers could store these huge amounts of data and could communicate with enough speed, the impracticality of working with huge data sets would remain. For instance, satellite measurements can often produce gigabytes or terabytes of data [5]. However, when used in the field, much of the data may be either irrelevant to the user or unnecessarily detailed. Simonsen and Hansen [6] provide the methodology of calculating the Hurst exponents using wavelet method.

The theory and applications of Hurst exponent have been vigorously studied by physicists, mathematicians and engineers alike in the last decade. In the beginning, its applications were limited to problems in image/signal analysis. But subsequently its applications are spread to diverse fields; to name a few, scientific computation, geophysics, meteorology, astrophysics, medical sciences, detection of abnormalities in mammogram to diagnose breast cancer; bioinformatics and computational biology such as DNA sequences, protein structure and microdata analysis. Time series analysis approach for analyzing real-world problems is quite popular. In the recent past, fractal dimensions have been focused to detect seasonalities and long time trends. Feature detection of electrocardiogram signals and proper understanding of financial and climatic time series are some of the challenging problems of the modern time which may be successfully studied by Hurst exponent and fractal dimensional analysis.

There are many processes which have random (stochastic) component, but also exhibit some predictability between an element and the next. In statistic, this is sometimes described as the autocorrelation (the correlation of data set with shifted version of the data set). The autocorrelation is one measure of whether a past value can be used to predict a future value. A random process that has some degree of autocorrelation referred to as long memory process (or long-range dependence). River flow exhibits this kind of long-term dependence. A hydrologist, named Hurst, studied Nile river flows and reservoir modeling (Mandelbrot and Richard [7]). The Hurst exponent to be computed using rescales range analysis ( $R/S$ ) and absolute moments methods for such kind of data such as rainfall and financial data takes name from its discover. In the recent past application of the Hurst exponent has been discovered in the study of financial and climate time series. The Hurst exponent is also directly related to the fractal dimension, which gives a measure of the roughness of a surface. The fractal dimension and their refinements have been used in diverse fields. The relationship between the fractal dimension,  $D$ , and the Hurst exponent  $H$ , is  $D = 2 - H$ . Carbone et al. [8] used the Hurst exponent analysis to study the long-term behavior of financial time series data to predict the stock trend in the future time domain. Rangrajan and Sant [9] used the fractal dimension analysis to study the climatic conditions of some parts of India. They developed predictability indices for different climatic zones using pressure, temperature and rainfall data.

The objective of the present paper is to study the long-term dependence of rainfall on pressure and temperature using Hurst exponent and fractal dimension estimation. The analysis further explores the predictability or dependence of rainfall on pressure and temperature using predictability indices.

## 2. Site and data description

The study utilizes daily average values of air temperature ( $T$  in  $^{\circ}\text{C}$ ), surface pressure ( $P$  in mb) and daily total rain (Rain in mm) from Abha, Al-Ahsa, Al-Baha, Makkah, Al-Wajh, Arar, Dhahran, Gizan, Nejran and Qaisumah to analyze the dependence of Rain on  $T$  and  $P$ . The location latitude, longitude and altitude are summarized in Table 1. This table also includes the data collection period for each station and number of data points used in the analysis.

The long-term variation of daily mean values of temperature and pressure is shown in Figs. 1 and 2, respectively. In these figures, the mean minimum and maximum values of temperature and pressure are based on the daily mean values. The maximum mean temperature of  $30.8^{\circ}\text{C}$  was observed in Makkah while a minimum of  $18.1^{\circ}\text{C}$  in Abha. Among coastal locations viz. Dhahran, Gizan and Al-Wajh, the mean temperature was found to be  $26.6^{\circ}\text{C}$ ,  $25.6^{\circ}\text{C}$  and  $25.0^{\circ}\text{C}$ , respectively. The mean temperature at Qaisumah and Nejran was  $25.4^{\circ}\text{C}$  and  $25.6^{\circ}\text{C}$  while at Al-Baha and Arar was  $22.2^{\circ}\text{C}$  and  $22.1^{\circ}\text{C}$ , respectively. The maximum temperature of  $42.0^{\circ}\text{C}$  of the daily mean values was found at Al-Ahsa during the data period used in the study. The minimum temperature of the daily mean values was found at Arar, i.e.,  $-0.7^{\circ}\text{C}$ . At Nejran and Qaisumah the minimum temperature of daily mean values was  $2.7^{\circ}\text{C}$ . The overall maximum mean air pressure was noticed at Dhahran and the minimum at Abha, as shown in Fig. 2.

Table 1  
Information about the locations used in this study

Location	Latitude	Longitude	Altitude (m)	Duration	Data points
Abha	18°13′	42°31′	2200	1983–1989	2039
Al-Ahsa	26°35′	48°10′	160	1983–1989	1280
Al-Baha	20°00′	41°30′	2130	1983–1989	2039
Makkah	21°25′	39°50′	286	1990–2004	5357
Al-Wajh	26°14′	36°26′	22	1991–2004	5112
Arar	30°54′	41°08′	542	1991–2004	5357
Dhahran	26°06′	50°10′	22	1991–2004	5357
Gizan	16°52′	42°35′	5	1991–2004	5357
Nejran	17°34′	44°14′	1275	1991–2004	5326
Qaisumah	28°20′	46°07′	359	1991–2004	5357

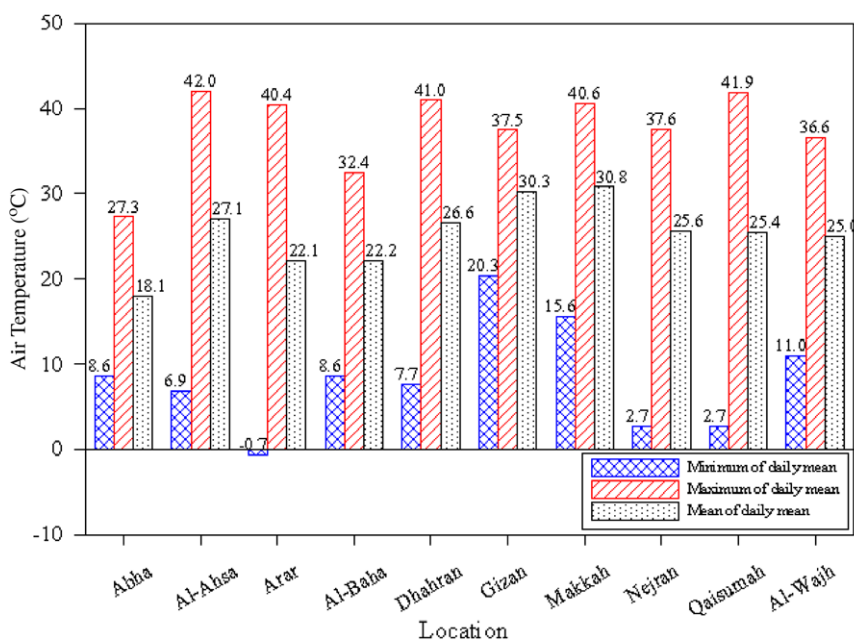


Fig. 1. Long-term variation of daily values air temperature.

The variation of daily mean time series data of air temperature, surface pressure and daily total rainfall is shown in Figs. 3–5, respectively. As seen from Fig. 3a–j, the temperature data at Abha [Fig. 3a], Al-Baha [Fig. 3d], Al-Wajh [Fig. 3g], Makkah [Fig. 3h] and Nejran [Fig. 3i] has smaller range of variation compared to that at Al-Ahsa [Fig. 3b], Arar [Fig. 3c], Dhahran [Fig. 3e] and Qaisumah [Fig. 3j]. The least range in the variation of temperature time series was observed at Gizan, as depicted in Fig. 3f. The daily variation in pressure values at all the meteorological stations, except Abha Al-Ahsa [Fig. 3a] and Al-Baha Al-Ahsa [Fig. 3d] was almost the same. Abha and A-Baha are the two hill stations and are very different from other locations due its geographical conditions. The total daily rain occurred at each station is shown in Fig. 5a–j. It is evident from these figures that relatively high rainfall took place at Abha, Arar, AL-Baha, Gizan and Makkah compared to that at Al-Ahsa, Dhahran, Al-Wajh, Nejran and Qaisumah.

### 3. Methodology

The Hurst exponent occurs in several areas of applied mathematics, including fractals and chaos theory, long memory processes and spectral analysis. Hurst exponent estimation has been applied in areas ranging from biophysics to computer networking. Estimation of the Hurst exponent was originally developed in hydrology. However, the modern techniques for estimating the Hurst exponent come from fractal mathematics. The mathematics and images derived

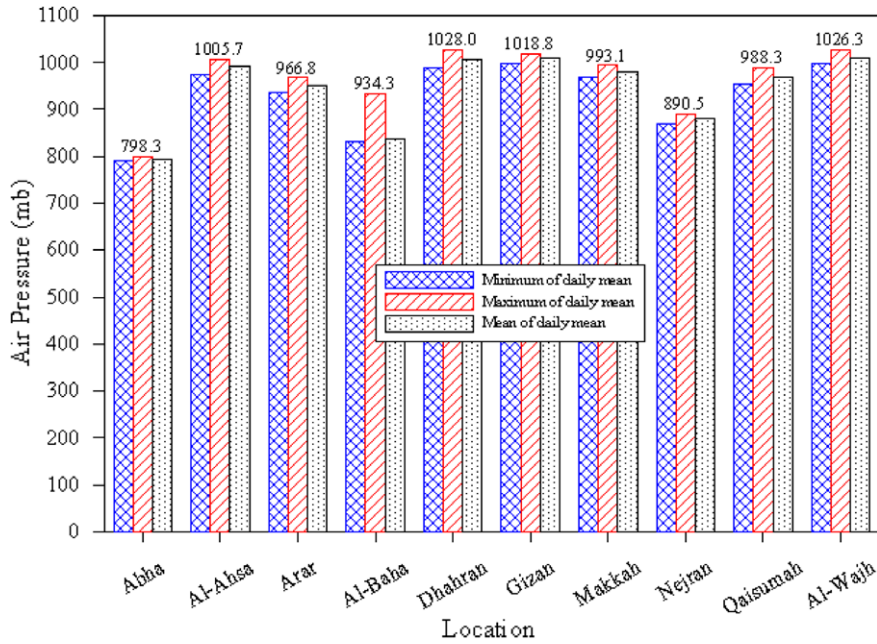


Fig. 2. Long-term variation of daily air pressure.

from fractal geometry exploded into the world the 1970s and 1980s. It is difficult to think of an area of science that has not been influenced by fractal geometry. The autocorrelation is one measure of whether a past value can be used to predict a future value. A random process that has some degree of autocorrelation referred to as long memory process (or long-range dependence). River flow exhibits this kind of long-term dependence. A hydrologist, named Hurst, studied Nile river flows and reservoir modeling [10]. The Hurst exponent to be computed using different methods for such kind of data such as rainfall and financial data takes name from its discover. In the recent past application of the Hurst exponent has been discovered in the study of financial and climate time series.

The values of the Hurst exponent range between 0 and 1. A value of 0.5 indicates a true random walk (a Brownian time series). In a random walk there is no correlation between any element and a future element. A Hurst exponent value  $H$ ,  $0.5 < H < 1$  indicates “persistent behavior” (e.g., a positive autocorrelation). A Hurst exponent value  $0 < H < 0.5$  will exist for a time series with “anti-persistent behavior” (or negative autocorrelation). The Hurst exponent is also directly related to the fractal dimension, which gives a measure of the roughness of a surface. The fractal dimension and their refinements have been used in diverse fields. The relationship between the fractal dimension  $D$ , and the Hurst exponent  $H$ , is  $D = 2 - H$ . The predictability indices for pressure ( $PI_P$ ), temperature ( $PI_T$ ) and rainfall ( $PI_R$ ) time series are calculated as follows:

$$PI_P = 2|D_P - 1.5|, \quad PI_T = 2|D_T - 1.5| \quad \text{and} \quad PI_R = 2|D_R - 1.5| \quad (1)$$

where  $D_P$ ,  $D_T$  and  $D_R$  are the fractal dimensions of pressure, temperature and rainfall temperature series, respectively. The climate predictability index is defined as the combination of the above predictability indices and is given as follows:

$$PI_C = (PI_P, PI_T, PI_R) \quad (2)$$

In Eq. (1), the fractal dimensions  $D$ 's are taken as the absolute value because the predictability increases in two cases when fractal dimension becomes less than 1.5 or when it becomes more than 1.5, as explained by Rangarajan and Sant [9]. In the former case, a persistence or correlation behavior is observed while in the later one an anti-persistence or anti-correlation behavior. In Eq. (2), if one of these indices come close to 0, then the corresponding process approximates the usual Brownian motion and is therefore unpredictable [10]. If it becomes close to 1, the process is said to be very predictable.

### 3.1. Autocorrelation function

The autocorrelation is one measure of whether a past value can be used to predict a future value. A random process that has some degree of autocorrelation referred to as long memory process A data set exhibits autocorrelation if value

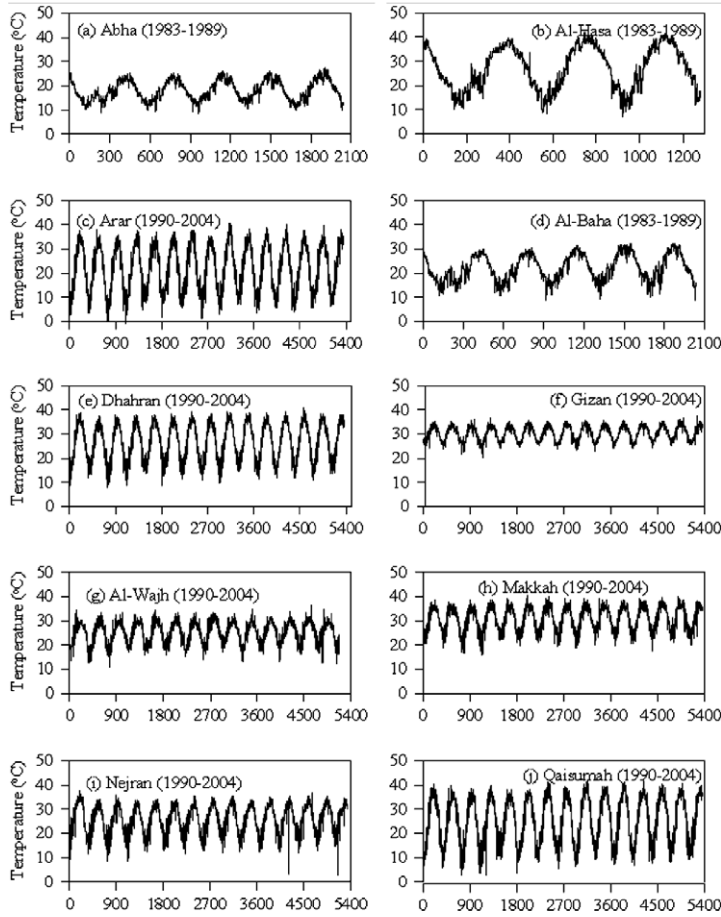


Fig. 3. Variation of daily mean values of temperature at various locations.

$x_i$  at time  $t_i$  is correlated with a value  $X_{i+d}$  at time  $t_{i+d}$  where  $d$  the time increment is in the future. In a long memory process autocorrelation decays over time and decay follows a power law namely

$$p(k) = Ck^{-\alpha} \tag{3}$$

where  $C$  is a constant and  $p(k)$  is the autocorrelation function with ( $lag_k$  autocorrelation defined below). For given  $X_1, X_2, \dots, X_n$  at time  $t_1, t_2, \dots, t_n$  the  $lag_k$  autocorrelation function is defined as

$$r_k = \frac{\sum_{i=1}^{n-k} (x_i - \bar{x})(x_{i+k} - \bar{x})}{\sum_{i=1}^n (x_i - \bar{x})^2} \tag{4}$$

where

$$\bar{x} = \frac{X_1 + X_2 + \dots + X_n}{n} \tag{5}$$

It may be remarked that in the definition the observations are equi-spaced. Autocorrelation is a correlation coefficient. However, instead of correlation between two different variables the correlation is between two values of same variable at time  $t_i$  and  $t_{i+k}$ . The autocorrelation function is being used to detect non-randomness in data and to identify an appropriate time series model if the data are not random. When autocorrelation is used to detect non-randomness, it is usually only the first ( $lag1$ ) autocorrelation that is of interest. When the autocorrelation is used to identify appropriate time series model, the autocorrelation are plotted for many lags.

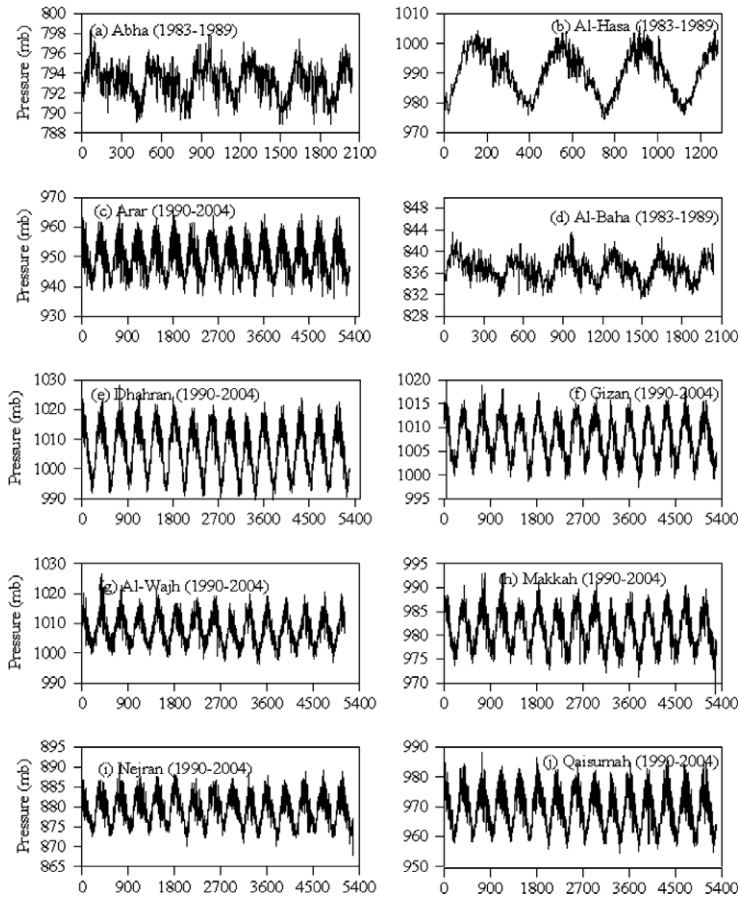


Fig. 4. Variation of daily mean values of pressure at various locations.

### 3.2. Estimation Hurst exponents using rescaled range (R/S) analysis

Consider an interval, or window, of length  $w$  in a trace or signal. Within this window, one can define two quantities namely;  $R(w)$ , the range taken by the values of  $y$  in the interval. The range is measured with respect to a trend in the window, where the trend is estimated simply as the line connecting the first and the last point within the window. This subtracts the average trend in the window.  $S(w)$ , the standard deviation of the first differences  $dy$  of the values of  $y$  within the window. The first differences of the  $y$ 's are defined as the differences between the values of  $y$  at some location  $x$  and  $y$  at the previous location on the  $x$ -axis

$$dy(x) = y(x) - y(x - dx) \quad (6)$$

where  $dx$  is the sampling interval, i.e., the interval between two consecutive values of  $x$ . A reliable measurement of  $S(w)$  requires data with a constant sampling interval  $dx$ , because the expected difference between successive values of  $y$  is a function of the distance separating them.  $S(w)$  in the rescaled range method is used to standardize the range  $R(w)$  to allow comparisons of different data sets. If  $S(w)$  is not used, the range  $R(w)$  can be calculated on data sets that have a non-constant sampling interval. The rescaled range  $R/S(w)$  is defined as

$$R/S(w) = \left\langle \frac{R(w)}{S(w)} \right\rangle \quad (7)$$

where  $w$  is the window length and the angled brackets  $\langle R(w) \rangle$  denote the average of a number of values of  $R(w)$ . The basis of the method is that, because of self-affinity, one expects the range taken by the values of  $y$  in a window of length  $w$  to be proportional to the window length to a power equal to the Hurst exponent  $H$ , i.e.,

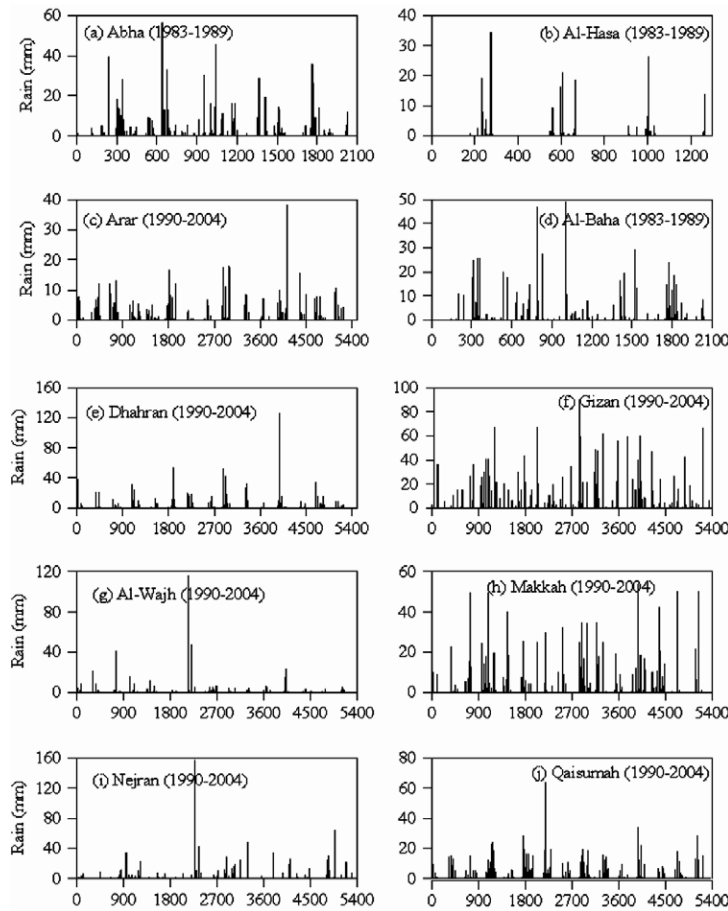


Fig. 5. Variation of daily mean values of rainfall at various locations.

$$R/S(w) = w^H \quad (8)$$

In practice, for a given window length  $w$ , one subdivides the input series in a number of intervals of length  $w$ , measures  $R(w)$  and  $S(w)$  in each interval, and calculates  $R/S(w)$  as the average ratio  $R(w)/S(w)$ , as in (2). This process is repeated for a number of window lengths, and the logarithms of  $R/S(w)$  are plotted versus the logarithms of  $w$ . If the trace is self-affine, this plot should follow a straight line whose slope equals the Hurst exponent  $H$ .

### 3.3. Estimation Hurst exponents using absolute value method

In this method an aggregated series  $X(m)$  is defined using different block sizes  $m$ . The log–log plot of the aggregation level versus the absolute first moment of the aggregated series  $X(m)$  should be a straight line with slope of  $H - 1$ , if the data are long-range dependent.

## 4. Results and discussion

The autocorrelation coefficients for temperature and rain for a number of time lags are shown in Figs. 6 and 7, respectively. The autocorrelation coefficients for all the meteorological stations show that temperature follows a well defined seasonal pattern, as can be seen from Fig. 6a–i. The seasonal patterns shown by autocorrelation functions are identical to the pattern formed by the temperature time series data shown in Fig. 3a–i. The autocorrelation function, not shown here, plotted for surface pressure followed the same seasonal trend shown by the pressure time series data

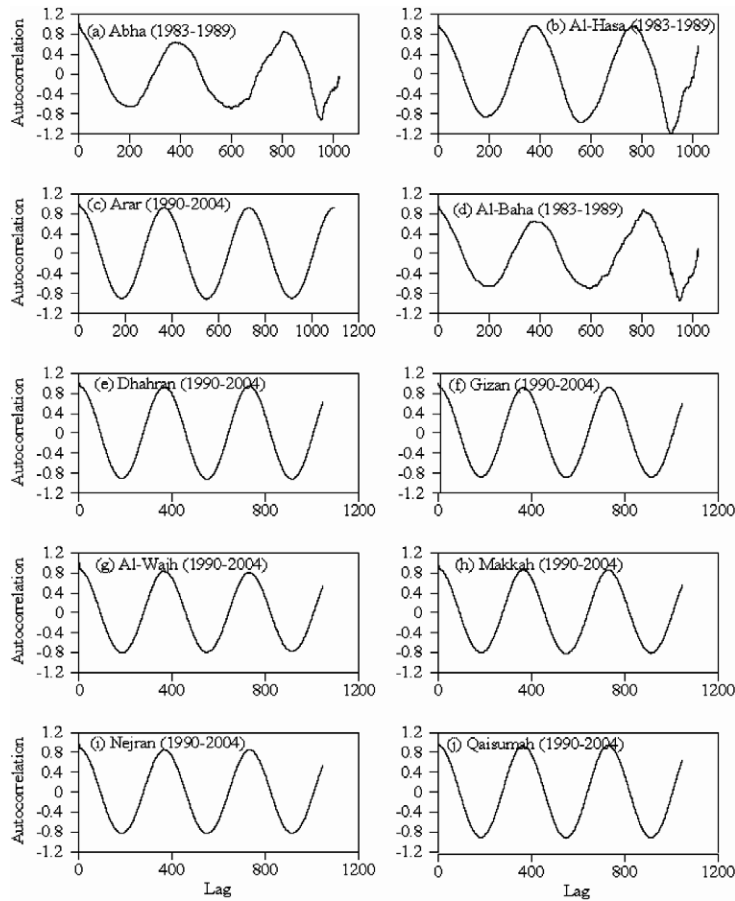


Fig. 6. Autocorrelation coefficients of air temperature time series with time lag.

plotted in Fig. 4a–i. The autocorrelation coefficient for total daily rainfall data for all the meteorological data collection stations is shown in Fig. 7a–i.

The Hurst exponents ( $H$ ) for pressure, temperature, rain, RH, WS, calculated using  $R/S$  analysis method, are summarized in Table 2. The SELFIS [9] software was used for the calculation of HE's. The  $H$  values for pressure, as seen from the first column of Table 2, lie well below 0.5 for all the stations. This indicates that pressure values in the future time step are not dependant on the previous values. The maximum  $H$  was observed for Al-Hasa pressure time series while the minimum of 0.17 for Arar. For the rest of the station  $H$  varied between 0.20 and 0.24. A value of 0.60 of  $H$  for temperature time series indicated that at Al-Wajh the temperature in future time domain highly depends on the previous values. For rest of the stations the  $H$  values were found to be less than 0.5 which indicates lesser dependence of future temperature values on the previous ones.

The  $H$  values for rainfall data were found to be greater than 0.5 for all the stations which is indicative of the dependence of future time step values on previous ones. A maximum of 0.71  $H$  value was found for rainfall data at Abha while a minimum of 0.59 for Al-Wajh. The  $H$  for relative humidity time series were also observed to be greater than 0.5 for all the stations, hence can be predicted in future time domain using the previous values. The maximum  $H$  of 0.7 were found for Nejran and Qaisumah while the minimum of 0.52 for Al-Wajh. Though the wind speed is highly unpredictable perimeter, the  $H$  values were found to be greater than 0.5 for all the time series data used in this study. This shows relatively higher dependence of wind speed in future time domain on the previous values.

The  $H$  values were also calculated using absolute moments method and are given in Table 2. For pressure and temperature time series, the absolute moment method resulted higher values of  $H$  compared to  $R/S$  analysis method. For relative humidity and rainfall time series,  $R/S$  method produced higher values of  $H$  compared to absolute moment method while in case of wind speed absolute moment method gave higher values.



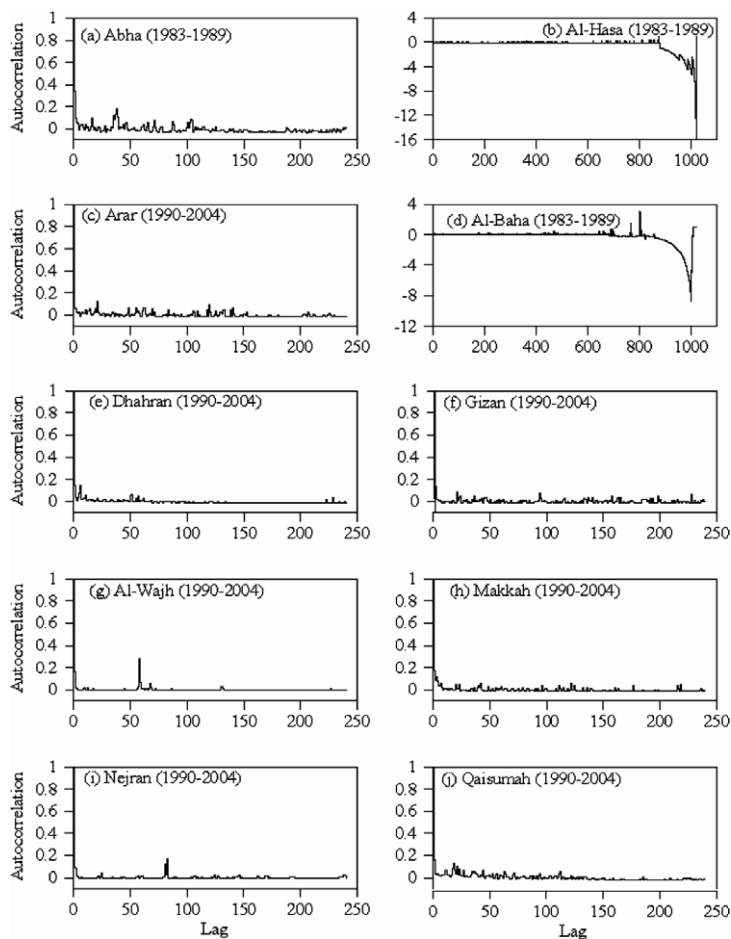


Fig. 7. Autocorrelation coefficients of daily total rainfall time series with time lag.

Table 2

Hurst exponents for nine locations

Station	Rescaled range analysis method					Absolute value method				
	PR	TP	Rain	RH	WS	PR	TP	Rain	RH	WS
Abha	0.23	0.34	0.71	0.66	0.60	0.54	0.64	0.49	0.54	0.58
Al-Ahsa	0.33	0.40	0.63	0.62	0.58	0.57	0.58	0.20	0.38	0.58
Al-Baha	0.24	0.33	0.67	0.62	0.61	0.66	0.61	0.52	0.57	0.57
Makkah	0.20	0.40	0.60	0.60	0.70	0.60	0.40	0.50	0.60	0.80
Al-Wajh	0.22	0.60	0.59	0.52	0.57	0.56	0.97	0.61	0.62	0.70
Arar	0.17	0.48	0.66	0.66	0.68	0.47	0.42	0.60	0.33	0.72
Dhahran	0.20	0.40	0.60	0.60	0.60	0.60	0.50	0.50	0.50	0.60
Gizan	0.30	0.23	0.60	0.40	0.60	0.50	0.50	0.50	0.60	0.70
Nejran	0.22	0.40	0.60	0.70	0.74	0.55	0.40	0.60	0.60	0.80
Qaisumah	0.21	0.45	0.70	0.70	0.70	0.55	0.50	0.60	0.50	0.80

The climate predictability index quantifies the predictability of three major components comprising the climate, i.e., pressure temperature and rainfall. The quantification is performed using a fractal dimensional analysis of the corresponding time series. In the present case, the climate predictability indices are calculated for 10 locations in the Kingdom of Saudi Arabia. If the fractal dimensions ( $D$ ), also known as surface roughness, for a particular time series is 1.5,

Table 3  
Predictability indices

Stations	PR	TP	Rain
Al-Wajh	0.56	0.20	0.18
Dhahran	0.60	0.20	0.20
Gizan	0.40	0.54	0.20
Abha	0.54	0.32	0.42
Al-Baha	0.52	0.34	0.34
Al-Ahsa	0.35	0.20	0.26
Makkah	0.60	0.20	0.20
Arar	0.66	0.04	0.32
Nejran	0.56	0.20	0.20
Qaisumah	0.58	0.10	0.40

we get an usual Brownian motion. This implies that there is no correlation between amplitude changes corresponding to two successive time intervals. Hence no trained in amplitude can be discerned from the time series and the process is said to be unpredictable. If the fractal dimension decreases to 1, the process becomes more and more predictable as it exhibits persistence. This simply means that the future trained is more likely to follow and established trend (Hsui et al., 1993). Further more, as the fractal dimension increases from 1.5 to 2.0, the process exhibits anti-persistence. In this case again the predictability increases.

In order to understand the predictability indices and the dependence of rain predictability index on pressure and temperature indices, the meteorological stations are regrouped into smaller groups as follows:

Group I: Comprising of coastal locations such as Al-Wajh on the North-West, Gizan on the south-west and Dhahran on the East coast.

Group II: Comprising of meteorological stations located in the South-West terrain area like Abha and Al-Baha.

Group III: Comprising of Al-Ahsa, Makkah, Arar, Nejran and Qaisumah in-land locations.

The climate predictability indices for all the locations in above defined groups calculated using fractal dimensions are summarized in Table 3. The  $PI$ 's given in table, were calculated using  $H$  obtained from  $R/S$  analysis method. At coastal locations (viz. Al-Wajh, Gizan and Dhahran) the precipitation/rainfall seems to be relatively independent of both the pressure and temperature predictability indices. In case of Gizan a decrease in  $PI_P$  and substantial increase in  $PI_T$  did not cause any change in  $PI_R$ . For Abha and Al-Baha region, the precipitation predictability index changed significantly from 0.42 to 0.34 though  $PI_P$  decreased from 0.54 to 0.52 and  $PI_T$  increased from 0.32 to 0.34, i.e., by an insignificant magnitude. This shows again, that at these two locations the precipitation is dependent both on the local pressure and temperature changes no matter how small are these changes.

From Al-Ahsa data, the  $PI_C$  was (0.35, 0.20, 0.26) while for Arar (0.66, 0.04, 0.37), as given in Table 3. Comparing the  $PI_C$  for two geographically extreme locations Al-Ahsa (East-South) and Arar (East-North) the  $PI_P$  increased significantly to 0.66 for Arar compared to 0.35 for Al-Ahsa while  $PI_T$  decreased to 0.04 for Arar compared to 0.20 for Al-Ahsa but the precipitation index  $PI_R$  increases from 0.37 to 0.26. This shows that at Arar the precipitation increases due to increase in  $PI_P$  and decrease in  $PI_T$ . At other in-land locations like Makkah, Nejran and Qaisumah the  $PI_P$  was almost the same in the range 0.56–0.60 while  $PI_T$  was 0.20 for Makkah and Nejran and 0.10 for Qaisumah. Since  $PI_P$  and  $PI_T$  were similar at Makkah and Nejran the precipitation index ( $PI_R$ ) was also the same, i.e., 0.20 as can be seen from Table 3. Hence the two locations have same time type of precipitation dependency on pressure and temperature predictability indices. But at Qaisumah a substantial decrease in  $PI_T$  of 50% seems to be responsible for the increase in  $PI_R$ , i.e., of 0.40. In this case the rainfall/precipitation was found to be more dependent on temperature predictability index compared to pressure.

## 5. Conclusions

The study of meteorological data from Abha, Al-Ahsa, Al-Baha, Makkah, Al-Wajh, Arar, Dhahran, Gizan, Nejran and Qaisumah in terms of autocorrelation, Hurst exponent, and climate predictability index resulted into following observations:

1. At Abha, Al-Hasa, Arar, Al-Baha, Dhahran, Gizan, Makkah, Nejran, Qaisumah and Al-Wajh the mean temperature was found to be 18.1 °C, 27.11 °C, 22.09 °C, 22.17 °C, 26.57 °C, 30.27 °C, 30.79 °C, 25.65 °C, 25.44 °C and 25.03, respectively. The surface pressure, in above order, was found to be 793.18 mb, 990.23 mb, 949.41 mb, 836.86 mb, 1006.62 mb, 1007.68 mb, 981.34 mb, 879.25 mb, 969.36 mb and 1007.88 mb, respectively.
2. The Hurst exponents value,  $H$  showed persistence behavior for rainfall, relative humidity and wind speed time series data with  $H > 0.5$  and anti-persistence for pressure and temperature time series data with  $H < 0.5$  for all locations.
3. The  $H$  values were obtained using two methods viz. the rescaled range Analysis ( $R/S$ ) as the absolute moments (ABM). It is really difficult, scientifically, to say which method is accurate than the others. Moreover as seen from its literature,  $R/S$  method has been utilized more often for estimates of  $H$ .
4. The climate predictability index could not establish the dependency of rainfall on pressure and temperature or on either of the predictability indices in general. Further analysis should be performed to establish the climate predictability index by dividing time series into seasonal series and further into different time spans.

### Acknowledgements

The author wishes to acknowledge the support of Research Institute of King Fahd University of Petroleum and Minerals, Dhahran, Saudi Arabia.

### References

- [1] Kurnaz ML. Application of detrended fluctuation analysis to monthly average of the maximum daily temperatures to resolve different climates. *Fractals* 2004;12(4):365–73.
- [2] Aboufadel E et al. *Discovering wavelets*. New York: John Wiley & Sons; 1999.
- [3] Daubechies I. *Ten lectures on wavelets*. Philadelphia: SIAM; 1992.
- [4] Foufoula-Georgiou Efi et al., editors. *Wavelets in geophysics*. San Diego: Academic Press; 1994.
- [5] Gerstner T. Multiresolution compression and visualization of global topographic data. *GeoInformatica* 2003;7(1):7–32.
- [6] Simonsen I, Hansen A. Determination of the Hurst exponent by use of wavelet transforms. *Phys Rev E* 1998;58:2779–87.
- [7] Mandelbrot BB, Richard LH. *The (mis) behavior of markets. A basic book*. New York: A Member of Pursues Book Group; 2004.
- [8] Carbone A, Castelli G, Stanley H. Time dependent Hurst exponent in financial time series. *Physica* 2004;A344(1–2):267–71.
- [9] Rangrajan G, Sant DA. Fractal dimension analysis of Indian climate dynamics. *Chaos, Solitons & Fractals* 2004;19:285–91.
- [10] Hurst HE, Black RP, Simaika YM. *Long-term storage: an experimental study*. London: Constable; 1965.